Journal of Alloys and Compounds 509 (2011) 3931–3936

Contents lists available at ScienceDirect

Journal of Alloys and Compounds

journal homepage: www.elsevier.com/locate/jallcom

The effect of heat treatment on mechanical properties and corrosion behavior of AISI420 martensitic stainless steel

A. Nasery Isfahany [a], H. Saghafian [a,*], G. Borhani [b]

[a] Iran University of Science and Technology, Iran
[b] University of Isfahan, Iran

ARTICLE INFO

Article history:
Received 8 June 2010
Received in revised form
22 December 2010
Accepted 23 December 2010
Available online 31 December 2010

Keywords:
Martensitic stainless steel AISI 420
Heat treatment
Fractography
Corrosion

ABSTRACT

Martensitic stainless steels are widely used for their good mechanical properties and moderate corrosion resistance. However, the need for superior properties in specific applications (e.g. steam generators, mixer blades, etc.) led to wide researches on the performance improvement of these steels. Heat treatment was recommended as one of the best ways to this regard hence the effects of astenitizing temperature and time, and tempering temperature on the microstructure, mechanical and corrosion properties of AISI420 have been studied. In the current work the experimental results showed that the austeitizing temperature significantly affects mechanical properties. The increase of tempering temperature led to precipitation of M_7C_3 and secondary hardening in the range of 400–500 °C. SEM micrographs of the fracture surfaces showed a mixed fracture mechanism (brittle and ductile) at 200 °C and 700 °C and brittle mechanism at 500 °C. The Polarization curves were not significantly affected by the increment of austenitizing temperature.

1. Introduction

Martensitic stainless steels (MMSs) are commonly used for manufacturing components with excellent mechanical properties and moderate corrosion resistance, so that they can work under high and low temperatures. Unlike other stainless steels, their properties could be changed by heat treatment; hence these steels usually are used for a wide range of applications like steam generators, pressure vessels, mixer blades, cutting tools and offshore platforms for oil extraction [1–3]. In the annealed condition (as received), MSSs have a microstructure containing spheroidized carbides in a ferritic matrix [4]. Since the material is metallurgically complex, meticulous control of heat treatment is necessary for formation of a fully martensitic structure without forming δ-ferrite and retained austenite. Depending on the composition and processing history, martensitic stainless steel consists of martensite, undissolved carbides and δ-ferrite. Therefore, for the given composition of the steel, the strength and corrosion resistance completely depend on the amount of carbon and other alloying elements in the austenite. In general, in the medium carbon martensitic stainless steels containing more than 0.2 wt.%, carbon totally dissolves in the matrix [5]. However, grain coarsening, decarburization and retention of austenite should be avoided. Furthermore, the presence of residual stress could obviously deteriorate the mechanical and corrosion properties. Applying an appropriate tempering temperature can relieve the stress and causes decomposition of new carbides. Thus, it is well known that the properties in martensitic stainless steels are strongly influenced by austenitizing and tempering treatment [6,7]. The aim of the present research is to analyze the effect of austenitizing and tempering on mechanical properties and electrochemical corrosion resistance based on the microstructure changes.

2. Experimental

The experimental steel was produced in a vacuum induction furnace. Molten steel was cast as cylindrical ingots. The chemical composition of the steel is given in Table 1.

The ingot was refined by the electroslag refining process. The refined ingots were hot forged between 900 and 1000 °C, annealed at 700 °C followed by air cooling. Blocks of suitable size were cut along longitudinal direction for the heat treatment experiments. Samples were austenitized at 980, 1015 and 1050 °C for 30, 60 and 120 min. All samples were tempered at 200 °C for 1 h. To determine the second hardening temperature range, tempering treatment was conducted in the range of 200–700 °C. Hardness measured on the samples for all heat treatment condition using Rockwell C scale. Room temperature tensile test and room temperature charpy V-notch impact test were carried out according to DIN-EN 10001-2 and DIN-EN 10045 standard respectively. For metallographic test, samples were polished and prepared in villela's reagent. Fracture surface of the impact test specimens were examined using scanning electron microscopy. EDS analysis was utilized to identify carbides decomposed at different tempering temperature. Finally, the influence of heat treatment parameters on the electrochemical behavior was evaluated.

* Corresponding author at: School of Metallurgy & Materials Engineering, Iran University of Science and Technology, Narmak, Farjam, Tehran 16876-13114, Iran. Tel.: +982177240344; fax: +98 2177240480.
E-mail address: Saghafian@iust.ac.ir (H. Saghafian).

0925-8388/$ – see front matter © 2010 Elsevier B.V. All rights reserved.
doi:10.1016/j.jallcom.2010.12.174

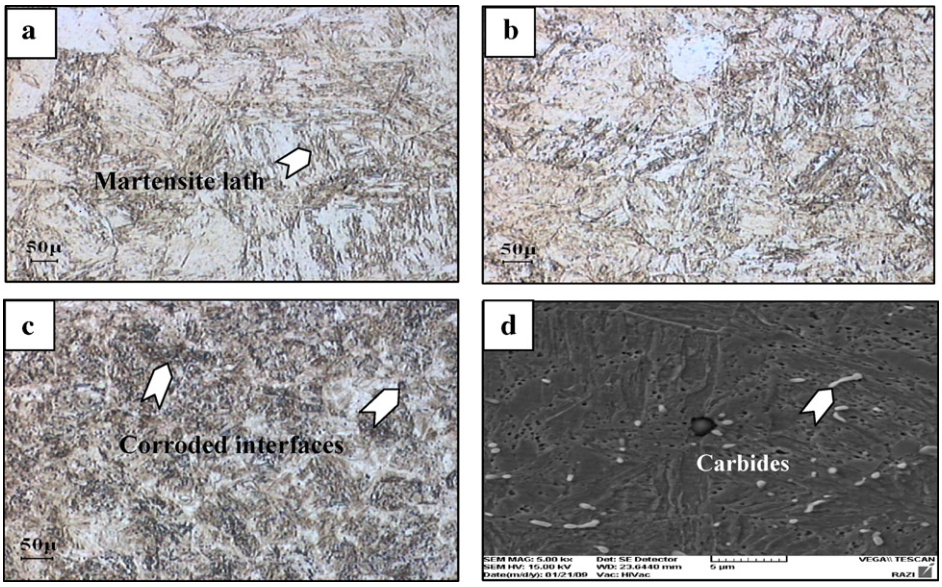

Fig. 1. Microstructure of the heat treated AISI 420, (a) 1050 °C, (b) 1015 °C, (c) 980 °C and (d) SEM micrograph at 980 °C.

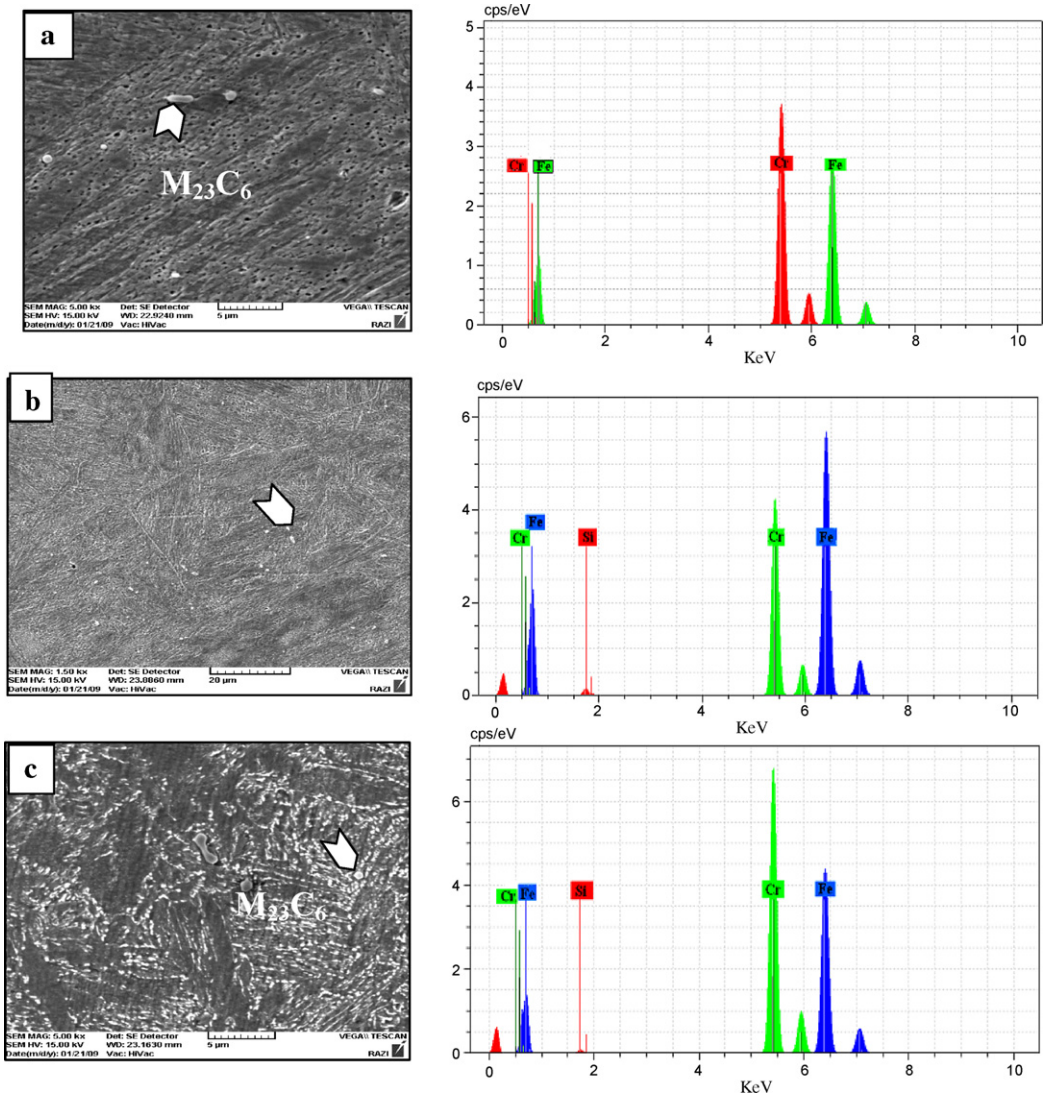

Fig. 2. EDS analysis of specimens tempered at (a) 200 °C, (b) 500 °C and (c) 700 °C.

Table 1
Chemical composition of AISI 420 martensitic stainless steel (wt.%).

%W	%V	%Al	%Cu	%Ni	%Mo	%Cr	%S	%P	%Mn	%Si	%C
0.04	0.02	0.012	0.11	0.2	0.06	12.98	0.004	0.019	0.46	0.32	0.22

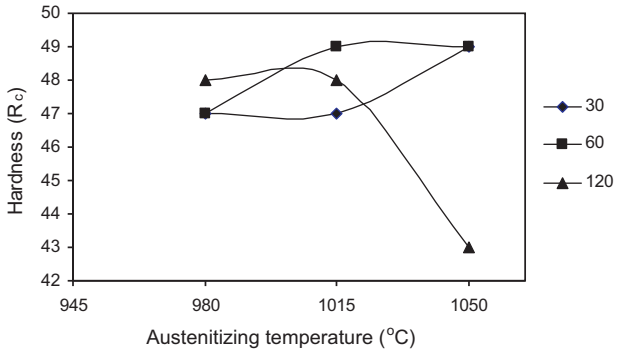

Fig. 3. Effect of austenitizing time and temperature on hardness.

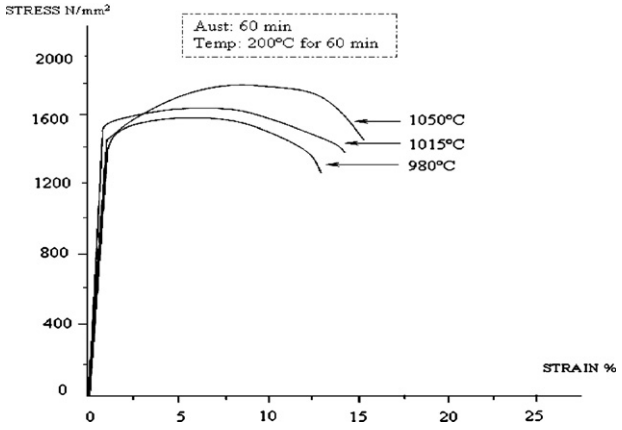

Fig. 4. Stress–strain curves at three austenitizing temperature (soaking time: 60 min).

3. Result and discussion

3.1. Microscopic evaluation

The optical and SEM micrographs of the AISI 420 austenitized at different temperature are shown in Fig. 1(a)–(d).

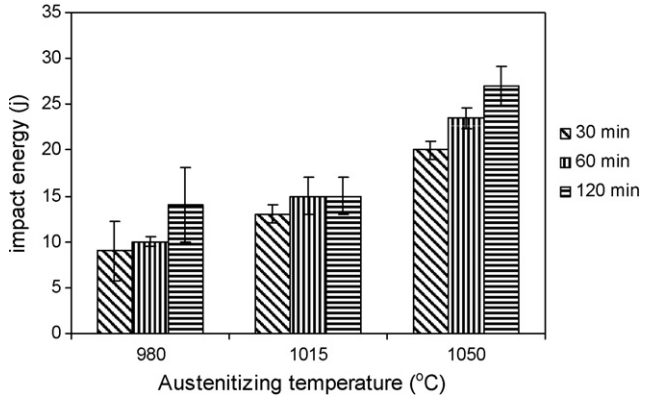

Fig. 5. Impact energy versus austenitizing time and temperature.

The microstructure of AISI 420 martensitic stainless steel in the annealed condition includes ferrite and $M_{23}C_6$ [4]. Depending on the austenitizing temperature, the amount of carbides in the matrix would be variable. After quenching, the lath martensite is the most common phase in the microstructure. In addition, fine carbides are visible especially at lower temperature. However, the amount of carbide decreased with the increment of austenitizing temperature from 980 to 1050 °C. Austenitizing time had a low effect on the microstructure. Fig. 2(a)–(c) shows the result of EDS analysis for specimens that were tempered at 200, 500 and 700 °C respectively. EDS results together with the results reported by Calliari et al. [8] on similar stainless steel showed that the identified carbides at 200, 500 and 700 °C could be $M_{23}C_6$, M_7C_3 and $M_{23}C_6$, respectively.

3.2. Austenitizing

Fig. 3 shows the effect of austenitizing time and temperature on hardness. In general, the high hardness is due to the homogonous distribution of lath martensite in the microstructure.

Variation of hardness can be attributed to the combination of two factors. First, the increase of the alloying elements such as chromium and carbon in the austenite with the increase of temperature and second, the presence of retained Austenite within lath martensite which usually increases with austenitizing temperature and time and has a detrimental effect on hardness. Combination of these factors led to the highest hardnesses in the specimens austenitized at 1050 °C. Tensile properties of heat treated specimens are shown in Fig. 4.

Maximum strength was acquired for the specimen austenitized at 1050 °C. The increase of the austenitizing temperature increases

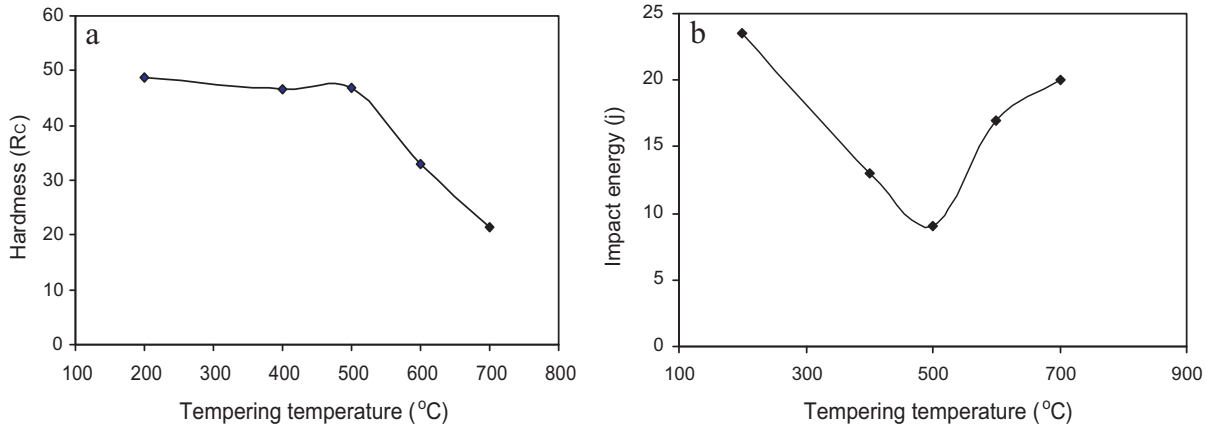

Fig. 6. (a) Hardness, (b) impact energy versus tempering temperature.

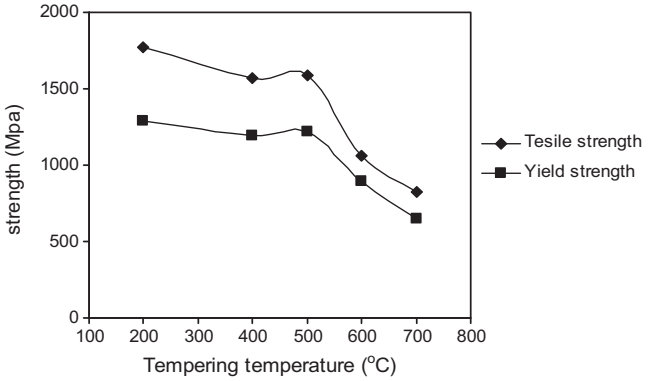

Fig. 7. Effect of tempering temperature on the tensile and yield strength.

the carbide dissolution in the matrix. Garcia de Andres et al. [9] showed that in the same stainless steel the increase of austenitizing temperature decreased carbides from 9.9% to 6.6%. The strength increment is resulted from the dissolution of $M_{23}C_6$ carbide in the matrix which increases the carbon supersaturation and lattice distortion of the martensite [10] together with the amount of twin boundaries and dislocations in the microstructure [11]. Garcia de Andres et al. [6] demonstrated that upon austenitizing in the range of 1000–1050 °C, grain growth remains to some extent constant due to the presence of the undissolved carbides in the austenite grain boundaries during heating. In this range of temperature, there was a moderate austenite grain growth and tensile strength was not greatly changed.

In Fig. 5 the impact energy as a function of austenitizing temperature for different times is shown. Impact energy increased with the increase of the austenitizing temperature. Three main reasons for improvement of the impact energy could be mentioned:

1 Increment of retained austenite within the lath martensite that absorbs the fracture energy [12].
2 Reduction of carbide volume fraction and their homogenous distribution.
3 Reduction of phosphorous in the grain boundaries. Among the various impurity atoms (tin, phosphorous, manganese, silicon) phosphorous has been found to be particularly detrimental to impact energy in 13% chromium martensitic stainless steel [1]. This detrimental impurity can be solved in the matrix, with increasing austenitizing temperature.

3.3. Tempering

The optimum strength and hardness were observed when austenitizing at 1050 °C for 60 min. This cycle was selected for the next tests. In Fig. 6(a), the hardness values of the specimens

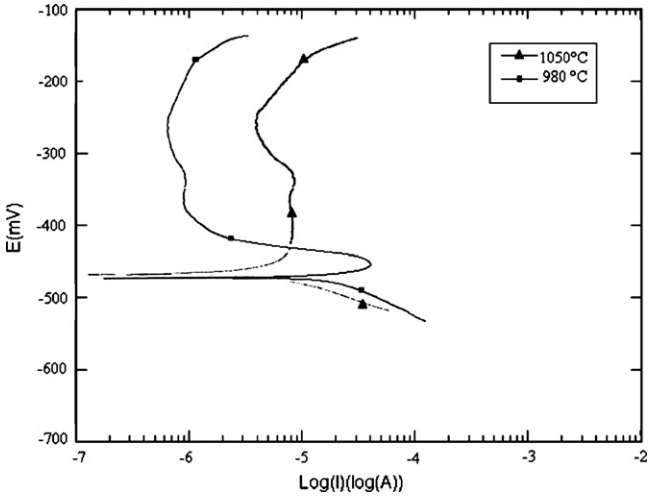

Fig. 9. Comparison between 980 °C and 1050 °C potensiostatic curves in AISI 420.

quenched and tempered at various temperatures are shown. As seen, hardness was almost constant for tempering temperatures ranging from 200 to 400 °C

Increasing hardness during tempering in the range of 400–500 °C can be attributed to the secondary hardening phenomenon. This is generally associated with the formation of M_7C_3 carbides within the martensite lath (Fig. 2). It can be also seen in Fig. 6(b) that hardness decreased when tempering at temperatures in the range of 500–700 °C. This Softening occurred when the M_7C_3 carbides started to coarsen and partially transform to $M_{23}C_6$ carbides illustrated in Fig. 2(c). The impact strength (Fig. 6(b)) decreased when tempering temperature increased from 200 to 500 °C so that the least impact strength observed at 500 °C. The highest impact energy at 200 °C could be attributed to the presence of retained austenite within the lath martensite absorbing fracture energy [12], and also to the lowest amount of carbide volume fraction and some detrimental elements such as phosphorous in the grain boundaries [1]. Therefore reduction of impact energy with increasing tempering temperature to 500 °C, could have been resulted from reducing the retained austenite volume fraction, increasing carbide particle and also reprecipitation of phosphorous at grain boundaries [1]. Impact strength increased again at 700 °C, because martensite tempered and a recovery took place in it. Impact strength at 200 and 700 °C is almost the same. The impact strength should have significantly improved with the tempering at 700 °C, but the presence of coarse carbide restricted the ductility, in spite of the presence of tempered martensite. Variations of tensile and yield strengths as a function of tempering temperature are shown in Fig. 7. As seen, strength reduced when tempering temperature increased from 200 °C to 400 °C. However,

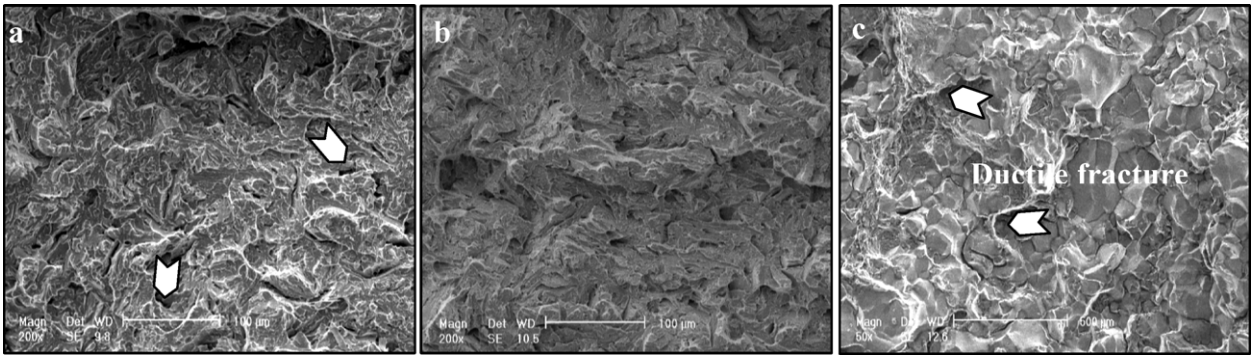

Fig. 8. SEM micrographs: austenitizing at 1050 °C for 60 min and tempered at (a) 200 °C, (b) 500 °C and (c) 700 °C.

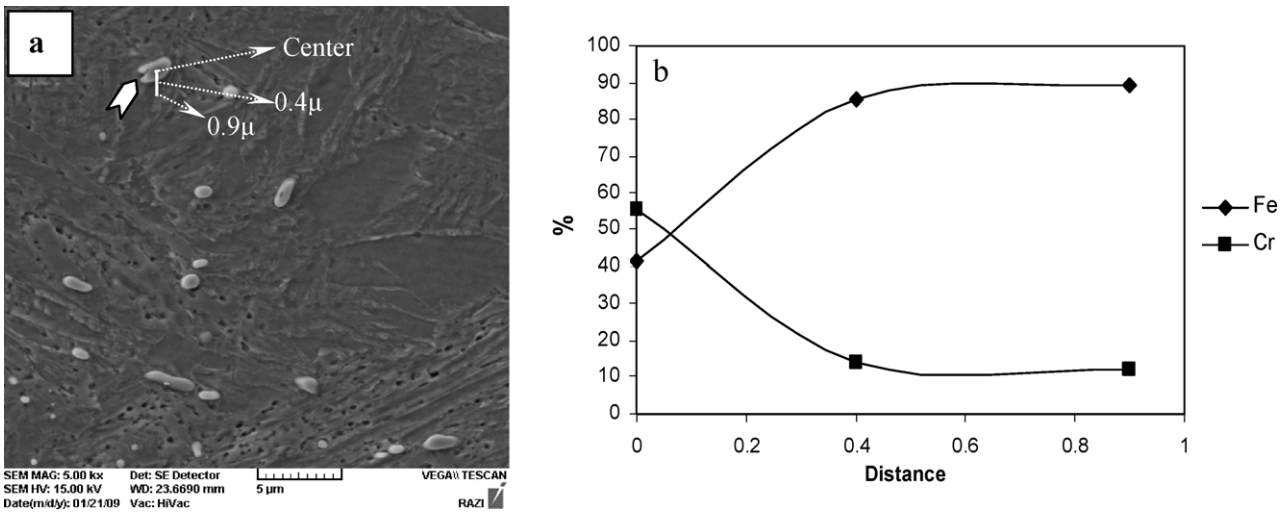

Fig. 10. (a) SEM micrograph, (b) iron and chromium percentage in various distance of carbides.

further increasing in tempering temperature to 500 °C resulted in an increased strength induced by a secondary strengthening phenomenon. As result, connection of micro cracks induced by tensile stress is retarded.

3.4. Fractography

SEM micrographs of the impact-test specimens fractured at ambient temperature are illustrated in Fig. 8. As shown, there is a negligible plastic deformation in all specimens especially in the specimens tempered at 500 °C. However, there are some plastic deformation places and micro-voids in specimens tempered at 200 °C and 700 °C. In fact, a mixture of ductile and brittle mechanisms is visible in these specimens. The fracture appearance appears mainly as the cleavage and river pattern or brittle features mixing with a little fibrous ductile region. More fibrous ductile features observed in specimens tempered at 700 °C. In addition, some voids are present in the fracture surface probably formed at the matrix/carbide interfaces.

3.5. Corrosion characteristic

Polarization curves (Fig. 9) in specimens austenitized at 980 and 1050 °C (tempered at 200 °C) showed a small difference in the I_{corr} and passive current density (PCD). Nevertheless, difference in PCD is more noticeable than I_{corr}. This difference in electrochemical behavior could be attributed to the dissolution of some alloying elements in the matrix. As explained above, since the carbide dissolution has increased with increasing the austenitizing temperature, the amount of some alloying elements such as chromium and carbon increased in the matrix. Dissolved chromium has significant effect on the reduction of I_{corr}. Meanwhile, dissolution of carbides in the matrix resulting in more homogenous microstructure is an important factor in reduction of I_{corr}. In spite of that, specimens austenitized at 1050 °C showed higher PCD than those austenitized at 980 °C which probably related to matrix carbon content. The effect of the matrix carbon content on PCD has been also confirmed by horovitz [13] and candelaria [10]. Horovitz has reported that PCD in stainless steels is usually increased with increasing matrix carbon content. In addition, the extra dissolved carbon could increase martensite lattice internal stresses having a deleterious effect on PCD [10].

EDS analysis (Fig. 10) of carbides in the microstructure resulted from heat treatment at 980 °C showed another fact. EDS analysis was carried out at different points over the line in this figure. Fig. 10(b) represents chromium and iron content in the carbide, in the matrix in center and at point 0.4 μm and 0.9 μm from the center of the carbide. From this figure, it is clear that almost all carbides in the matrix are undissolved carbides and precipitated carbides are in minority. So, there is no chromium depletion in the matrix and passive layer easily formed on the surface. Therefore, due to the lowest carbon content in the matrix and absence of chromium depletion regions, passive layer can form easier in the 980 °C austenitized specimen.

4. Conclusions

The effect of heat treatment parameters on the mechanical properties and electrochemical behavior was studied and the following conclusions were drawn:

(1) The maximum hardness (about 50 R_C), strength (about 1900 MPa) and impact toughness (about 30 J) are resulted from austenitizing at1050 °C.
(2) Secondary hardening took place at tempering temperature in the range of 400–500 °C due the formation of M_7C_3 within martensite lathes. Softening occurred when the M_7C_3 carbides start to coarsen and partially transform to $M_{23}C_6$ carbides.
(3) A good combination of mechanical properties can be achieved by the austenitizing at 1050 °C and tempering at 200 °C for 60 min.
(4) Fractographs of tempered specimens at 200 and 700 °C presented a mixture of ductile and brittle behavior. The fracture appearance appeared mainly as the cleavage and river pattern of brittle fracture mixing with a little fibrous ductile region.
(5) I_{corr} and PCD varied with austenitizing temperature. This variation could be attributed to the effect of some dissolved elements such as chromium and carbon.

References

[1] S.K. Bhambri, Journal of Material Science 21 (1986) 1741–1746.
[2] D.A. Porter, Phase Transformation in Metals and Alloys, 2nd ed., Chapman & Hall, Von Nostraned Reinhold, 1981.
[3] M.C. Tsai, C.S. Chiou, J.S. Du, J.R. Yang, Material Science and Engineering A 332 (2002) 1–10.
[4] J.S. Dubey, S.A. Vadekar, J.K. Chakravatry, Journal of Nuclear Materials 254 (1998) 271–274.
[5] R.A. Lula, Stainless Steel American Society for Metal, 2nd ed., McGraw-Hill, New York, 1986.

[6] C. Garcia de Andres, L.F. Alvarez, V. Lopez, Journal of Material Science 33 (1988) 4095–4100.
[7] J.Y. Park, Y.S. Park, Material Science and Engineering A 232 (2006) 1–4.
[8] I. Calliari, M. Zanesco, M. Dabala, K. Brunelli, E. Ramous, Material & Design (2006) 1–5.
[9] C. Garcia de Andres, G. Caruana, L.F. Alvarez, Material Science and Engineering A 241 (1998) 211–215.
[10] A.F. Candelaria, Journal of Material Science 22 (2003) 1151–1153.
[11] J.G. Gonzalez-Rodriguez, G. Bahena-Martinez, V.M. Salinas-Bravo, Material Letters 43 (2000) 208–214.
[12] H. Nakagawa, T. Miazaki, Journal of Material Science 34 (1999) 3901–3908.
[13] M.B. Horovitz, F. beneduce Neto, A. Garbogini, A.P. Tschiptschin, ISIJ International 36 (1996) 840–845.